International Journal of Mass Spectrometry 304 (2011) 25–28

Contents lists available at ScienceDirect

International Journal of Mass Spectrometry

journal homepage: www.elsevier.com/locate/ijms

Theoretical study of the effect of ion trap geometry on the dynamic behavior of ions in a Paul trap

I. Ziaeian*, S.M. Sadat Kiai, M. Ellahi, S. Sheibani, A. Safarian, S. Farhangi

Nuclear Science and Technology Research Institute (NSTRI), Nuclear Science Research School, A.E.O.I., PO Box 14155-1339, Tehran, Iran

ARTICLE INFO

Article history:
Received 21 December 2010
Received in revised form 8 March 2011
Accepted 8 March 2011
Available online 17 March 2011

Keywords:
Ion confinement
Paul ion trap
Ion trap geometry
Fractional mass resolution
Six-order Runge–Kutta method

ABSTRACT

The influence of the ion trap geometrical shape, ring and end-cap electrodes, on the dynamical behavior of the confined ions is studied. At first by considering the geometrical parameter $z_0 = (1/\sqrt{n})r_0$, where n is a real number, in the quadrupole potential, we solve Mathieu's differential equation for the first stability region using the six-order Runge–Kutta method. The numerical results show that, for a given ion trap mode i.e., rf only mode, the electrode geometry plays an important role both in higher ion mass confinement range and in a higher fractional mass resolution $m/\Delta m$.

1. Introduction

The quadrupole ion trap (QIT) is widely used in industries and laboratories for its capability of confining of gaseous ions for a period of time and as a mass filter of considerable mass range and variable mass resolution. This device consists of three electrodes; two of them are end-cap electrodes and the third is a ring electrode that has an internal hyperbolic surface. The ring electrode is located symmetrically between two end-cap electrodes as shown in Fig. 1. Here r_0 is the radius of the ring electrode in the central horizontal plane and $2z_0$ is the separation of the two end-cap electrodes measured along the axis of the ion trap.

The QIT can confine ions for a period of time in the rf field depending on the experimental conditions. To obtain the ideal quadrupolar potential, the relationship between the dimensions r_0 and z_0 is taken as $r_0^2 = 2z_0^2$ [1–3]. In this case the asymptotes bisect the gaps between the ring electrode and the end-cap electrodes at high values of r and z.[1]

Any changes in $r_0^2 = 2z_0^2$ relation will affect the form of the quadrupolar potential field. In this article, we have changed the geometrical shape of QIT by entering the parameter $z_0 = (1/\sqrt{n})r_0$ in the quadrupole field to survey the behavior of ion motion by solving the Mathieu differential equation. The results show that, for the specified lab conditions, one can obtain a higher fractional mass resolution.

2. Theory

2.1. Ion movement

The electrodes of the ion trap are truncated to obtain a practical working but this truncation introduces higher order multipole component to the potential [4]:

$$\varphi(r,z) = C_0^0 + C_1^0 z + C_2^0\left(\frac{1}{2}r^2 - z^2\right) + C_3^0 z\left(\frac{3}{2}r^2 - z^2\right) + C_4^0\left(\frac{3}{8}r^4 - 3r^2z^2 + z^4\right) + \dots \quad (1)$$

The C_n^0 coefficients for $n = 0$, 1, 2, 3 and 4 correspond to monopole, dipole, quadrupole, hexapole and octapole components, respectively. For a quadrupole ion trap, only the coefficients corresponding to $n = 0$ and $n = 2$ are non-zero. In this article, we have only discussed the influence of the stretched ion trap on the behavior of ions in a quadrupole 3D trap. For the stretched ion trap the asymptotes to the end-cap electrodes do not coincide with those for the ring electrode.

* Corresponding author. Tel.: +98 21 88221076.
E-mail address: iziaeian@aeoi.org.ir (I. Ziaeian).

[1] R.D. Knight, personal communication, 2004.

1387-3806/$ – see front matter © 2011 Elsevier B.V. All rights reserved.
doi:10.1016/j.ijms.2011.03.004

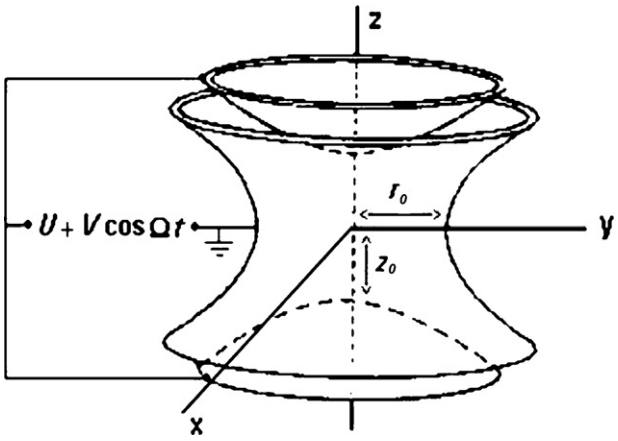

Fig. 1. A schematic view of a Paul trap.

The general equation of the potential within the stretched ion trap ($r_0^2 \neq 2z_0^2$) is defined as follows [2]:

$$\phi(r,z) = \frac{\phi_0(r^2-2z^2)}{r_0^2+2z_0^2} + \frac{2\phi_0 z_0^2}{r_0^2+2z_0^2} \tag{2}$$

When $r_0^2 = 2z_0^2$ is substituted into Eq. (2) we obtain the quadrupole potential in the 3D ion trap:

$$\varphi(r,z) = \frac{\varphi_0(r^2-2z^2)}{2r_0^2} + \frac{\varphi_0}{2} \tag{3}$$

By applying a combination of dc and a radio frequency (rf) ac voltages to the end-cap and ring electrodes of the stretched ion trap, namely $U+V\cos\Omega t$, Eq. (2) becomes:

$$\phi(r,z) = \frac{(U+V\cos\Omega t)(r^2-2z^2)}{r_0^2+2z_0^2} + \frac{2(U+V\cos\Omega t)z_0^2}{r_0^2+2z_0^2} \tag{4}$$

where V stands for zero to peak voltage, $V_{0\text{-p}}$, $\Omega = 2\pi f$ denotes the angular frequency of the ac voltage, and f is the frequency in Hz. The electric field components of the stretched QIT, z and r, are expressed as:

$$E_z = -\left(\frac{d\phi}{dz}\right)_r = \frac{4(U+V\cos\Omega t)z}{r_0^2+2z_0^2} \tag{5}$$

$$E_r = -\left(\frac{d\phi}{dr}\right)_z = -\frac{2(U+V\cos\Omega t)r}{r_0^2+2z_0^2} \tag{6}$$

The set of differential equations governing the motion of an ion with mass m and charge e, in QIT can be written [4,5]:

$$\frac{d^2z}{d\xi^2} + (a_z - 2q_z\cos 2\xi)z = 0 \tag{7}$$

$$\frac{d^2r}{d\xi^2} + (a_r - 2q_r\cos 2\xi)r = 0 \tag{8}$$

For the stretching of the ion trap, the trapping parameters are calculated using the actual values of z_0 and r_0 as follows [2,4]:

$$a_z = -2a_r = -\frac{16eU}{m(r_0^2+2z_0^2)\Omega^2} \tag{9}$$

$$q_z = -2q_r = \frac{8\,\text{eV}}{m(r_0^2+2z_0^2)\Omega^2} \tag{10}$$

$$\xi = \frac{\Omega t}{2} \tag{11}$$

The relationship between the parameters r_0 and z_0 is not considered in these formula. Historically we see that the relationship $r_0^2 = 2z_0^2$ has been selected to form the ideal quadrupolar potential.

2.2. Expression of fractional resolution

The resolution of a Paul ion trap mass spectrometer is a function of the mechanical accuracy such as alterations in radius of the ring electrode in the central horizontal plane Δr_0, and in our case a new parameter Δz_0 that is the change of closest distance from center of the QIT to the end-cap electrodes and the stability performance of the electronics devices such as variations in voltage amplitude ΔV and the rf frequency $\Delta\Omega$ [6].

To obtain a formula for the fractional resolution, we recall the stability parameter q:

$$q = \frac{8\,\text{eV}}{m(r_0^2+2z_0^2)\Omega^2} \tag{12}$$

By taking the partial derivative with respect to variables of the stability parameter q, we pick up a formula for the fractional resolution $m/\Delta m$, as follows:

$$\begin{aligned}\Delta m = {} & \left(\frac{8e}{q(r_0^2+2z_0^2)\Omega^2}\right)|\Delta V| + \left(\frac{16\,\text{eV}}{q(r_0^2+2z_0^2)\Omega^3}\right)|\Delta\Omega| \\ & + \left(\frac{16r_0\,\text{eV}}{q(r_0^2+2z_0^2)^2\Omega^2}\right)|\Delta r_0| + \left(\frac{32z_0\,\text{eV}}{q(r_0^2+2z_0^2)^2\Omega^2}\right)|\Delta z_0| \\ & + \left(\frac{16r_\circ eV}{q\left(r_\circ^2+2z_\circ^2\right)^2\Omega^2}\right)\left|\Delta r_\circ\right| + \left(\frac{32z_\circ eV}{q\left(r_\circ^2+2z_\circ^2\right)^2\Omega^2}\right)\left|\Delta z_\circ\right|\end{aligned} \tag{13}$$

Division of Eqs. (12) and (13) gives the final equation for the fractional resolution:

$$\frac{m}{\Delta m} = \left\{\left|\frac{\Delta V}{V}\right| + 2\left|\frac{\Delta\Omega}{\Omega}\right| + \frac{2r_0^2}{r_0^2+2z_0^2}\left|\frac{\Delta r_0}{r_0}\right| + \frac{4z_0}{r_0^2+2z_0^2}\left|\Delta z_0\right|\right\}^{-1} \tag{14}$$

Eq. (14) shows that, if two traps have the same time variation in amplitude and frequency but different geometry in the radial and axial dimension, we will have different fractional mass resolution.

3. Results and discussion

3.1. Ion trajectory

By entering the $z_0 = (1/\sqrt{n})r_0$ parameter in Eq. (2) and solving the Mathieu differential equation, we study behavior of $^{20}Ne^+$. Figs. 2–4 depict the ion trajectories for a typical geometrical conditions $n = 1.5$, 2 and 3, respectively, with $r_0 = 10$ mm, $f = 1$ MHz, $U = 0$, $V = 100$ V and $\xi = 100$. These figures show that the ion trajectory is more restricted in the r and z directions when we put the lowest value of n in $z_0 = 1/\sqrt{n}r_0$.

3.2. Stability diagram in U–V plane

With solving simultaneously by Eqs. (7) and (8), the stability diagrams are obtained in the a–q plane. The first stability region for the stretched quadrupole ion trap in a–q plane was computed using the six-order Runge–Kutta method. Fig. 5 shows the first stability region in a–q plane for different geometrical conditions, when n in $z_0 = 1/\sqrt{n}r_0$ parameter is 1.5 and 3. The corresponding results for an ideal quadrupole ion trap for $n = 2$ are also included in Fig. 5 in order to compare them at a glance. As a conclusion, one can see that the first stability region in a–q plane by increasing the size of n

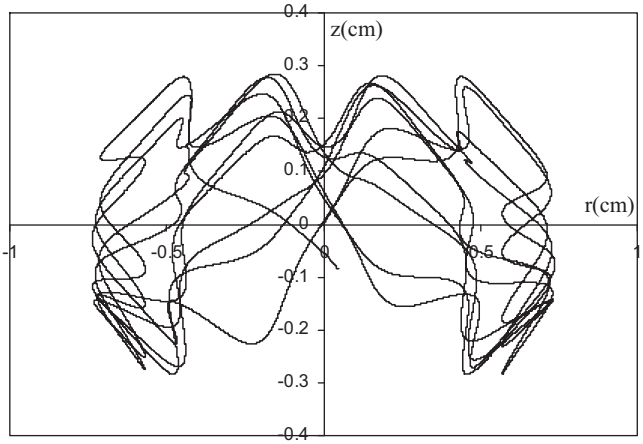

Fig. 2. The trajectory of a $^{20}Ne^{+}$ when the relation between r_0 and z_0 is $r_0 = \sqrt{1.5}z_0$ for $f = 1$ MHz, $U = 0$, $V = 100$ V, $r_0 = 10$ mm and $\xi = 100$.

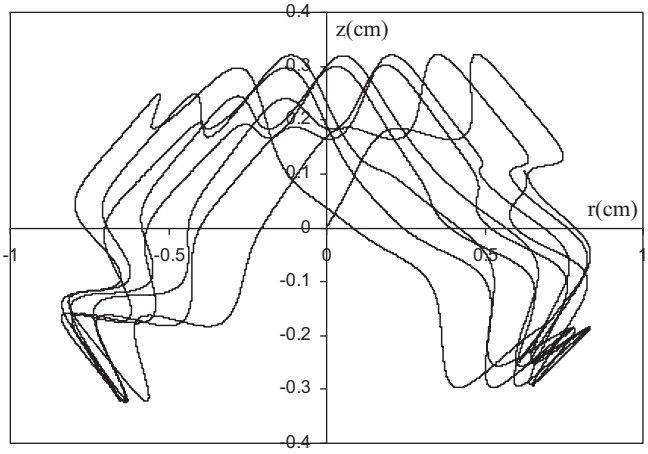

Fig. 3. The trajectory of a $^{20}Ne^{+}$ when the relation between r_0 and z_0 is $r_0 = \sqrt{2}z_0$ for $f = 1$ MHz, $U = 0$, $V = 100$ V, $r_0 = 10$ mm and $\xi = 100$.

is significantly stretched as compared with ideal quadrupole case ($n = 2$), whereas by decreasing the size of n, the first stability region in the a–q plane is reduced as compared with an ideal QIT.

By entering $z_0 = (1/\sqrt{n})r_0$ parameter in Eqs. (9) and (10), and solving the Mathieu's differential equation according to U and V

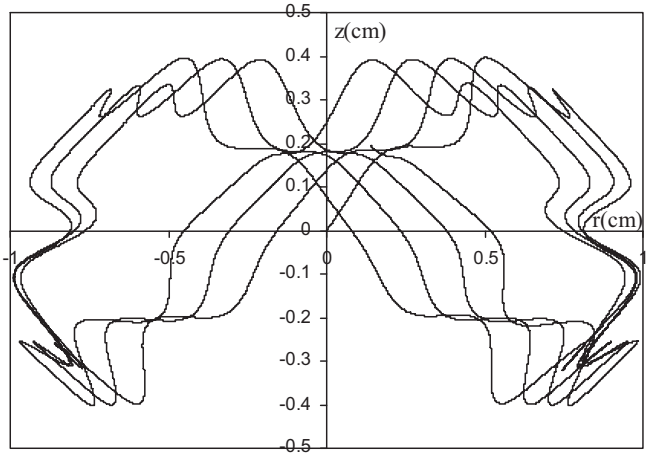

Fig. 4. The trajectory of a $^{20}Ne^{+}$ when the relation between r_0 and z_0 is $r_0 = \sqrt{3}z_0$ for $f = 1$ MHz, $U = 0$, $V = 100$ V, $r_0 = 10$ mm and $\xi = 100$.

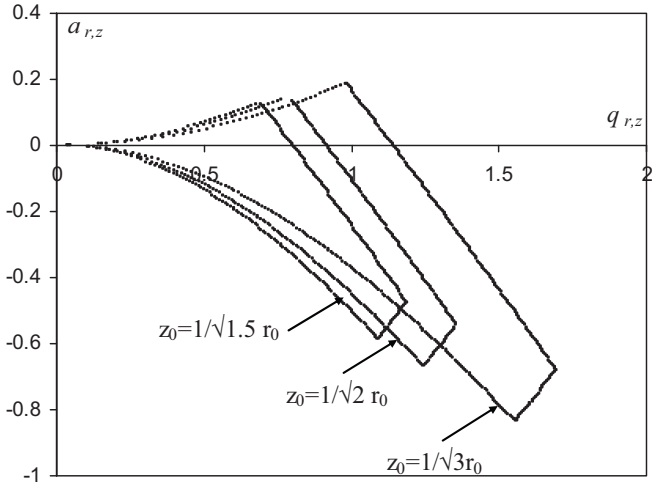

Fig. 5. The first stability region for a Paul trap in the a–q plane when the n in $z_0 = (1/\sqrt{n})r_0$ is 1.5, 2 and 3, respectively. The region with $z_0 = (1/\sqrt{2})r_0$ is plotted for QIT.

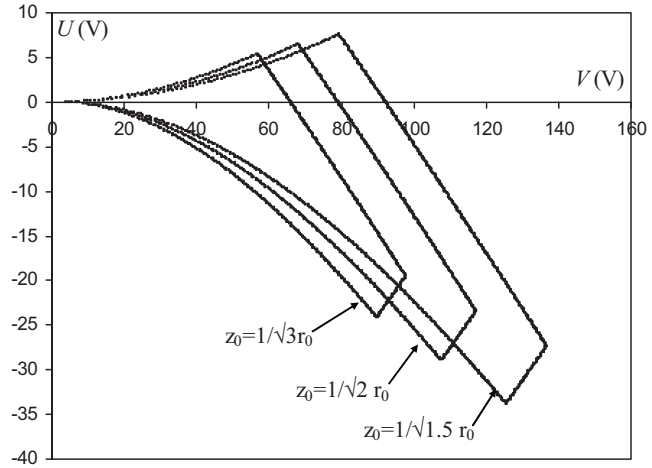

Fig. 6. The first stability diagram in the U–V plane for $^{20}Ne^{+}$ for $r_0 = 10$ mm and $f = 650$ KHz with $n = 1.5$, 2 and 3, respectively.

parameters, we can obtain the first stability diagram for an specified ion in the U–V plane, using the six order Runge–Kutta method. Also, one can get more information to separate ions from this diagram.

Based on the first stability diagram in the U–V plane, one can adjust the conditions of the system such as direct and alternating voltage to select a specific ion. Fig. 6 shows the stability diagram in U–V plane with $r_0 = 10$ mm and $f = 650$ KHz for $^{20}Ne^{+}$ with $n = 1.5$, 2 and 3, respectively. Comparing Figs. 5 and 6 with each other, one can see that, when n increases, the first stability region in a–q plane is larger; in contrast the first stability region in U–V plane is smaller. This means that, smaller traps have higher a and q values for a given voltage.

Fig. 7 presents the evolution of the fractional mass resolution according to n and the following conditions: As in Refs. [7,8] the inner radius of the hyperboloid ring is $r_0 = 10$ mm, the geometrical uncertainties $\Delta r_0 = 3 \times 10^{-3}$ mm with $\Delta r_0/r_0 = 3 \times 10^{-4}$, the rf frequency uncertainties $\Delta\Omega/\Omega = 10^{-7}$ and the voltage uncertainties $\Delta V/V = 10^{-4}$. We have taken arbitrary different uncertainties values for parameter ΔZ_0 from 10^{-3} to 10^{-4} mm. The dotted line is plotted for $n = 2$ where the relationship between r_0 and z_0 is $z_0 = r_0/\sqrt{2}$ in ideal QIT. From Fig. 7, it can be seen that the mass resolution for lower n is higher than $n = 2$ for a special ΔZ_0. It is noteworthy that for the large changes in n (n up to 10) the field will be highly

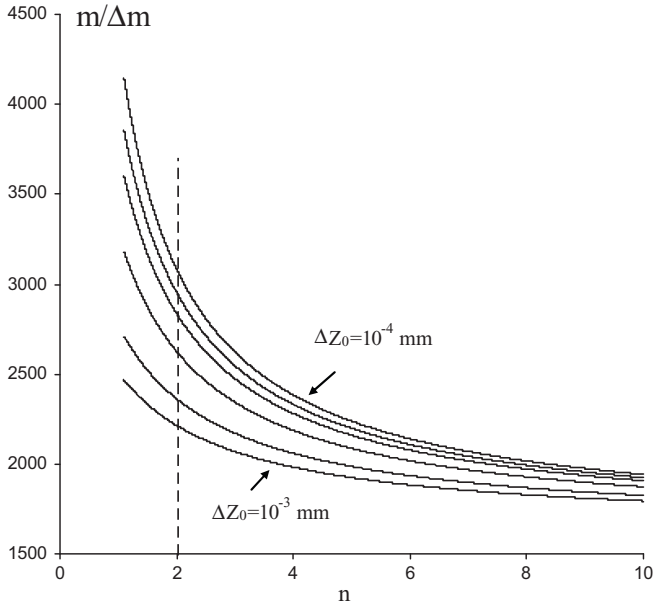

Fig. 7. The fractional mass resolution as a function of n. The dotted line is plotted for $n = 2$ where the relationship between r_0 and z_0 is $z_0 = r_0/\sqrt{2}$.

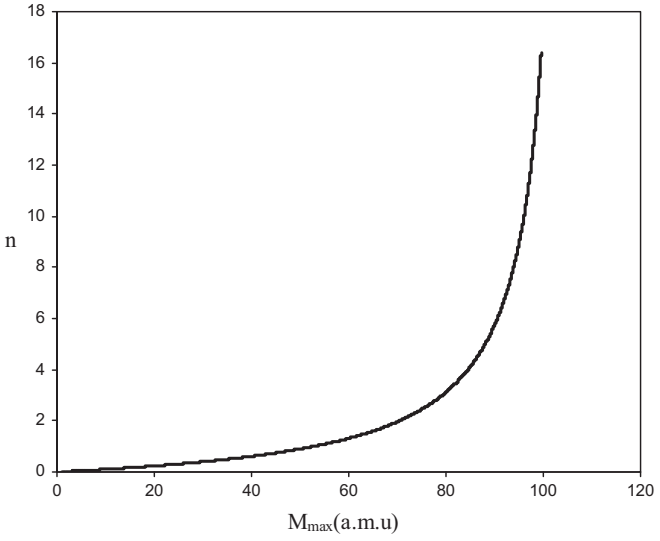

Fig. 8. The diagram of surrounded highest mass ions according to value of n in relation. $z_0 = (1/\sqrt{n})r_0$.

distorted and the simplistic conclusions from Eq. (14) are unlikely to apply.

3.3. Confined highest mass ions

The highest confined mass (m/z) in QIT depends on the trap's dimension, rf frequency and amplitude of rf voltage. If the trap's dimension and rf frequency remains constant, the relation depends on the maximum of the voltage amplitude and the highest value of the q_z parameter, that is $q_z = 0.908$. For the charge state $z = 1$, the maximum of the trapped ion mass according to Eq. (10) is calculated as follows:

$$m_{\max} = \frac{8\,\text{eV}}{0.908(r_0^2 + 2z_0^2)\Omega^2} \tag{15}$$

When entering $z_0 = (1/\sqrt{n})r_0$ in to Eq. (15) and using $r_0 = 10$ mm, $V = 200$ V and $f = 650$ KHz, Fig. 8 is obtained, indicating the variation of the n as a function of highest confined ion mass. Fig. 8 shows that the highest mass that can be confined for a given voltage increases with n because increasing the amount of n will reduce the size of z_0 and therefore will increase the q values for a given voltage and hence can confine higher masses. So, by keeping a constant experimental condition, hence one can confine the highest masses, only by changing the trap geometrical size.

4. Conclusion

In this article we worked on the stretched Paul trap and achieved significant results. The dynamical behavior of ions in the trap, the stability diagrams and the fractional mass resolution will change due to changes in the trap geometry. Since the size of r_0 is constant, reducing the size of n in $z_0 = (1/\sqrt{n})r_0$ parameter, leads to an increase of the distance between end-cap to center of trap, compared to ideal Paul trap ($r_0^2 = 2z_0^2$), we obtain the following results.

The ion trajectory is more restricted in the r and z directions, the first stability region in a–q plane is compacted, the first stability diagram in U–V plane for a typical ion is enlarged and the fractional mass resolution is higher. These may improve the performance of mass measurements in ion traps.

References

[1] R.F. Wuerker, H. Shelton, R.V. Langmuir, J. Appl. Phys. 30 (1959) 342.
[2] R.E. March, J.F.J. Todd, Quadrupole Ion Trap Mass Spectrometry, 2nd ed., Wiley, New Jersey, 2005, pp. 50–58.
[3] I. Ziaeian, H. Noshad, J. Mass Spectrom. 289 (2010) 1–5.
[4] R.E. March, J. Mass Spectrom. 32 (1997) 351–369.
[5] P.H. Dawson, Quadrupole Mass Spectrometry and Its Applications, AIP, New York, 1995 (originally published in 1976 by Elsevier Publishing Company, Amsterdam).
[6] O.J. Orient, A. Chutjian, Rev. Sci. Instrum. 73 (2002) 2157.
[7] O.J. Orient, A. Chutjian, Rev. Sci. Instrum. 74 (2003) 2936.
[8] S.M. Sadat Kiai, J. Mass Spectrom. 247 (2005) 61–66.